Physica Scripta

RECEIVED
12 July 2022

REVISED
16 October 2022

ACCEPTED FOR PUBLICATION
3 November 2022

PUBLISHED
16 November 2022

PAPER

A comparative study of new generic wormhole models with stability analysis via thin-shell

Faisal Javed[1], **Sobia Sadiq**[2], **G Mustafa**[1,*] **and Ibrar Hussain**[3]

[1] Department of Physics, Zhejiang Normal University, Jinhua 321004, People's Republic of China
[2] Department of Mathematics, Division of Science and Technology, University of Education, Lahore, Pakistan
[3] School of Electrical Engineering and Computer Science, National University of Sciences and Technology, H-12, Islamabad, Pakistan
[*] Author to whom any correspondence should be addressed.

E-mail: faisaljaved.math@gmail.com, sobia.sadiq@ue.edu.pk, gmustafa3828@gmail.com and ibrar.hussain@seecs.nust.edu.pk

Keywords: wormhole, exotic matter, modified gravity, thin-shell, stability analysis

Abstract

This analysis is devoted to exploring the interesting aspects of wormhole geometry. The energy conditions are checked for two different new generic shape functions, which satisfy the required wormhole properties. The presence of exotic matter is confirmed due to the violation of the energy conditions in the background of $f(R, T)$ gravity as well as in the general relativity case. The traversable wormholes respecting the null energy conditions can be realized in both considered frameworks. A thin-shell around a wormhole geometry with two different generic shape functions is obtained by using the cut and paste approach taking Schwarzschild spacetime as an exterior manifold. The stability of thin-shell is explored with linearized perturbation along the equilibrium shell radius. Stable regions and the position of the expected event horizon depend on the choice of physical parameters. It is concluded that the number of expected event horizons increases for the second shape function.

1. Introduction

A wormhole (WH) is a speculative region of spacetime that behaves like a shortcut connection between distinct regions of spacetime through a tunnel. A traversable WH provides a shortcut path having a minimal surface area between two points dubbed as WH throat through which a moving observer attempting to cross the WH tunnel falls into the singularity. Wormholes were described by Misner and Wheeler [1] as solutions of the Einstein field equations. To avoid the WH throat shrinking, the first traversable WH is introduced by Morris and Thorne [2]. To preserve their geometry, these WH solutions must meet the flare-out condition in which a thin layer of an exotic matter (violating the averaged null energy constraints) causes repulsion against the WH throat collapsing. The elimination of an event horizon allows observers to journey across both universes through the flat faces of a traversable WH, which is one of its most distinguishing features.

An essential characteristic of traversable WHs that suggests the presence of exotic matter necessary for their stability and existence is the violation of the weak and null energy constraints. Visser [3] presented a suitable approach to building a thin-shell WH structure by reducing the amount of exotic matter which allows free movement across the cosmos. The stable characteristics of traversable WHs while minimizing the violation of the null energy condition (EC) are investigated by Shinkai [4]. By choosing a suitable configuration for the WH, Visser *et al* [5] found that the violation of the null energy requirement can be minimized. Later, the stability regions of WH solutions are studied by Hayward and Bouhmadi-López *et al* [6]. In the study of WH solutions supported by generic equations of state, Parsaei and Rastgoo [7] showed that different types of equations of state have a great impact to reduce the null EC violation. Additionally, they discovered that the solutions fulfill the asymptotical flatness criterion and are also consistent with large-scale observational data.

According to some cosmic data, a period of accelerated expansion of the Universe is currently occurring, which is thought to be caused by an unusual energy source known as dark energy [8]. The phantom energy, Chaplygin gas, quintessence, and tachyon matter have all been investigated as potential sources of exotic matter at the WH throat.

Shushkov [9] formed static spherically symmetric WH solutions in the background of the phantom type of matter distribution which is considered a source of exotic matter. Lobo [10] explored the physical configuration of phantom WH geometry and traversable WHs are developed with the van der Waals quintessence in [11].

The most spectacular and effective approaches to revealing the hidden characteristics of the cosmos and supporting the cosmic expansion are said to be alternative gravity theories. The function of curvature invariant is added to or substituted for in the geometric component of the Einstein-Hilbert action to create these theories. Modified theories of gravity have drawn a lot of interest in the analysis of the current behavior of the Universe. The most straightforward strategy in this context is the $f(R)$ theory (R is the Ricci scalar), which has been extensively employed to investigate dark energy and the Universe's continuing expansion [12]. Without violating the required energy constraints, Lobo and Oliveira [13] developed the WH solutions in the $f(R)$ theory. Eiroa and Aguirre [14] investigated the stability of thin-shell spherical Lorentzian WHs in $f(R)$ theory in the background of electromagnetic field by using symmetry preserving perturbation. In the framework of Einstein-Maxwell-dilaton theory, Övgün and Jusufi [15] formed a charged spherically symmetric dyonic thin-shell WH and demonstrated that the stable domain of the dyonic thin-shell WH can be increased in terms of electric charge, dilaton charge as well as magnetic charge. Mazharimousavi [16] demonstrated that thin-shell WH cannot be formed in the black hole spacetime solution of charged $f(R)$ theory.

The geometrical configuration and stability of traversable WHs were investigated by Lobo *et al* [17] in the context of Palatini $f(R)$ gravity. It is found that thin-shell WHs constructed from RN BH are more stable than Schwarzschild BH. Using the Rastall gravity and anisotropic fluid distribution, Lobo *et al* [18] developed thin-shell WHs for static black holes. They determined the stability of WHs filled with various bulk sources and analyzed that stable regions of developed structures through effective potential are modified due to the Rastall parameter. Hassan *et al* [19] investigated the stability of WH solutions with two particular shape functions in $f(Q)$ gravity where Q denotes the non-metricity tensor. For the power-law $f(R)$ model, Capozziello *et al* [20] found traversable WHs with two specific shape functions. Recently, the phantom traversable WH geometries in Rastall gravity are developed by Javed *et al* [21]. They also determined the stable configuration of the thin shell with a speed of sound parameter and the physical features of the shell.

This modified $f(R)$ theory was further generalized by incorporating the idea of curvature-matter coupling. These theories are non-conserved with an additional force that alters the path of the particle. These modified approaches play a key role to study cosmic mysteries. The minimal coupling is introduced as $f(\mathfrak{R}, T)$ theory [22]. WH solutions in the region of this theory can be found from the associated field equations with different $f(R, T)$ models. Houndjo *et al* [23] used $f(R, T) = f_1(R) + f_2(T)$ and reconstructed various cosmological models. Shamir [24] formulated exact solutions of Bianchi type V spacetime in $f(R, T)$ gravity via constant deceleration parameter (yielding non-singular model) and variation law of Hubble parameter (yielding singular model). They calculated the physical quantities for evaluated models. Yousaf *et al* [25] investigated the compact object's evolution using structure scalars in the framework of $f(R, T)$ gravity and showed that evolutionary stages can be examined by modified scalar functions. Yousaf *et al* [26] discussed the stability as well as the physical existence of anisotropic WH solutions even when the exotic matter is not present. The $f(R, T) = f(R) + \lambda T$ model is used to develop WH structure in [27]. Moraes and Sahoo [28] discovered WH solutions that fulfill the energy constraints in the vicinity of the exponential $f(R, T)$ theory. The charged WH solutions in $f(R, T)$-extended theory is developed by Moraes *et al* [29] and Mandal *et al* [30] examined the energy conditions for $f(R, T) = R + f(T)$ gravity with a hybrid type of shape function. Sharif *et al* [31–35] explored the stability of various thin-shell WHs in GR and developed WH geometries in different modified theories of gravity. Traversable WH structures are developed in traceless $f(R, T)$ gravity by Sahoo *et al* [36]. By taking the model $f(R, T) = \lambda T + R + \alpha R^2$, Mishra and Sharma [37] obtained WHs using a hybrid form of shape function. Yousaf *et al* [38] observed a vacuumcavity around the center of symmetry for static fluid configuration admitting hyperbolically symmetric structure and imposed the condition of the stiff equation of state as well as conformal flatness to formulate several models.

The most intriguing cosmic entity that can be created in general relativity is the time-like thin-shell in spherically symmetric static spacetimes. In 1966, Israel [39] published a fundamental study that established a concrete framework for creating time-like shells in general by gluing two distinct manifolds at the position of the thin shell. Self-gravitating thin-shells are the solutions of a given gravitational theory describing two regions separated by an infinitesimally thin region where the matter is confined. The Randall-Sundrum brane world scenario to the gravitational collapse [40], shells around black hole solutions [41], matchings of cosmological solutions [42], and the evolution of bubbles and domain walls in cosmological settings [43] are all examples of how the Darmois-Israel thin shell formalism, a fundamental tool in Classical General Relativity, has found extensive applications in the literature. Many researchers have developed thin-shell by using cut and paste approach in the background of different interior and exterior manifolds, i.e., thin-shell (taking inner flat exterior BH geometry) [44, 45], thin-shell WHs (through the matching of two equivalent copies of BH geometries) [46, 47], gravastars (through joining of inner de Sitter and outer BH spacetime) [48, 49]. An interesting application to WH physics was done in [50], where Frolov and Novikov demonstrated that if one of the WH mouths is inserted in an external gravitational field, for instance, a thin shell is placed around one of the traversable WH mouths, the Killing vector field is well-defined locally but does not exist globally, enabling the transformation of the WH into a time machine. A similar concept for gravastar is used by Mazur and Mottola [48], where an interior region is replaced with de Sitter core and a phase transition is considered at event horizon $2M$. Lobo [51] determined surface stresses on the thin shell from the interior solution of a spherically symmetric traversable WH to a particular outer vacuum solution at a junction interface. Additionally, he investigated the constructed geometry's stability and dynamical behavior using surface stresses. Using a cut-and-paste method, Garcia *et al* [52] studied the stability of thin-shell structures derived from WH geometries and discovered that exotic matter significantly affects stable configuration. By assuming barotropic EoS, Forghani *et al* [53] developed an asymmetric thin-shell from two traversable WHs with various redshift functions. By merging a traversable WH with standard BHs (Bardeen and Hayward BHs), Sharif and Ashraf [54] created athin-shell structure and studied its stability as well as dynamics. These research articles motivate us to develop a thin-shell around traversable WH in the background of the modified theory of gravity. Then, we explored the stability of the developed thin-shell by using linearized radial perturbation at the equilibrium shell radius.

This paper is devoted to studying. In section 2, the $f(R, T)$ gravity is explored and a modified version of field equations are calculated. In the same section 2, new generic WH solutions are presented. All the energy conditions are provided in the next section 3. In section 4, thin-shells around calculated WHs configurations are discussed. The stability analysis through radial linear perturbation is made for both generic WH models in section 5. Finally, we conclude our results in the last section.

2. $f(R, T)$ gravity and wormhole geometry

The action of modified $f(R, T)$ gravity theory is provided as:

$$S = \frac{1}{16\pi}\int f(R,\ T)\sqrt{-g}\,d^4x + \int L_m\sqrt{-g}\,d^4x, \tag{1}$$

where L_m is the Lagrangian density. One can get the following equation by taking the variation of the above action:

$$\begin{aligned}8\pi.T_{\mu\nu} - f_T(R,\ T)T_{\mu\nu} - f_T(R,\ T)\Theta_{\mu\nu} = f_R(R,\ T)R_{\mu\nu} - \frac{1}{2}f(R,\ T)g_{\mu\nu}\\ + (g_{\mu\nu}\,\Box - \nabla_\mu\nabla_\nu)f_R(R,\ T).\end{aligned} \tag{2}$$

Now, by contracting the above equation, we have the following expression:

$$8\pi T - f_T(R,\ T)T - f_T(R,\ T)\Theta = f_R(R,\ T)R + 3\,\Box\, f_R(R,\ T) - 2f(R,\ T). \tag{3}$$

These two above equations involve the operator ∇, which is known as covariant derivative and $\Box$, which is known as d'Alembert operator. Further, $f_R(R, T)$ and $f_T(R, T)$ correspond to the function derivative with respect to R and T respectively, while the tensor $\Theta_{\mu\nu}$ is given as:

$$\Theta_{\mu\nu} = \frac{g^{\alpha\beta}\delta T_{\mu\nu}}{\delta g^{\mu\nu}} = -2T_{\mu\nu} + g_{\mu\nu}L_m - 2g^{\alpha\beta}\frac{\partial^2 L_m}{\partial g^{\mu\nu}\partial g^{\alpha\beta}}, \tag{4}$$

where $T_{\mu\nu}$ is a usual energy momentum tensor. By taking the help from [55], we suppose that L_m depends only on the metric components $g^{\alpha\beta}$, so we obtain energy momentum tensor as:

$$T_{\mu\nu}^{(m)} = -\frac{2}{\sqrt{-g}}\frac{\delta(\sqrt{-g}L_m)}{\delta g^{\mu\nu}} = g_{\mu\nu}L_m - \frac{2\partial L_m}{\partial g^{\mu\nu}}. \tag{5}$$

It is interesting to mention that an extra force depends on the form of the matter lagrangian [56]. It was discussed in [57] that by taking $L_m = p$, with p being the amount of the total pressure, the extra force vanishes. On the other hand, more natural forms for L_m, such as $L_m = -\rho$, with ρ being the energy density, are more generic, in the sense that they do not imply the vanishing of the extra force. In current study, we are working with the matter Lagrangian is $L_m = -\rho$. Hence, equation (4) can be revised as

$$\Theta_{\mu\nu} = -2T_{\mu\nu} - \rho g_{\mu\nu}. \tag{6}$$

Now, by using the equation (3) in equation (2), we have the following final relation for field equations:

$$\begin{aligned}f_R(R,\ T)G_{\mu\nu} = (8\pi + f_T(R,\ T))T_{\mu\nu} + [\nabla_\mu\nabla_\nu f_R(R,\ T)\\ - \frac{1}{4}g_{\mu\nu}\{(8\pi + f_T(R,\ T))T + \Box\, f_R(R,\ T) + f_R(R,\ T)R)\}].\end{aligned} \tag{7}$$

A static and spherically symmetric spacetime metric representing WH geometry is given as:

$$ds^2 = -e^{2\Phi(r)}dt^2 + \left(1 - \frac{b(r)}{r}\right)^{-1}dr^2 + r^2d\theta^2 + r^2\sin^2\theta d\phi^2, \tag{8}$$

where $\Phi(r)$ is the red-shift function and $b(r)$ is the shape function. The WH throat joins two asymptotic regions, i. e., $b(r_0) = r_0$. The flaring-out requirement, $b'(r) < 1$, which should valid at or near the throat, must be satisfied by the shape function $b(r)$. The metric functions must obey the requirements $\Phi(r)$ and $b(r)/r$ tend to zero as r approaches to ∞ to have asymptotically flat geometries. For the current analysis, we are fixing $\Phi(r) = Constant$, i.e., $\Phi' = 0$. The anisotropic source of matter is defined via energy-momentum tensor as:

$$T_{\zeta\eta} = \rho\upsilon_\zeta\upsilon_\eta + p_r\chi_\zeta\chi_\eta + (\upsilon_\zeta\upsilon_\eta - g_{\zeta\eta} - \chi_\zeta\chi_\eta)p_t, \tag{9}$$

where υ_ζ denotes the 4-velocity vector of $\upsilon^\zeta = e^{-\Phi(r)}\delta_0^\zeta$ and $\chi^\zeta = \sqrt{1 - \frac{b(r)}{r}}\delta_1^\zeta$, which must satisfy the conditions $\upsilon^\zeta\upsilon_\zeta = -\chi^\zeta\chi_\zeta = 1$. Now by using equation (8) and equation (9) in equation (7), we have following expressions for energy density and pressure components:

$$\frac{b'}{r^2} = \frac{X}{f_R(R, T)} + \frac{(8\pi + f_T(R, T))}{f_R(R, T)}\rho, \tag{10}$$

$$\begin{aligned} -\frac{b}{r^3} = &-\frac{X}{f_R(R, T)} + \frac{(8\pi + f_T(R, T))}{f_R(R, T)}p_r \\ &+ \frac{1}{f_R(R, T)}\left(1 - \frac{b}{r}\right)\left[\left(f_R{}''(R, T) - f_R{}'(R, T)\frac{b'r - b}{2r^2(-b/r + 1)}\right)\right], \end{aligned} \tag{11}$$

$$-\frac{-b + b'r}{2r^3} = \frac{8\pi + f_T(R, T)}{f_R(R, T)}p_t + \frac{1}{f_R(R, T)}\left(-\frac{b}{r} + 1\right)\frac{f_R{}'(R, T)}{r} - \frac{X}{f_R(R, T)}, \tag{12}$$

where

$$X \equiv X(r) = \frac{1}{4}(T(8\pi + f_T(R, T)) + f_R(R, T)R + \Box f_R(R, T)). \tag{13}$$

Ricci scalar for spacetime, which is given in equation (8) is

$$R = \frac{2b'}{r^2}, \tag{14}$$

and

$$\Box f_R(R, T) = \left(1 - \frac{b}{r}\right)\left[-f_R'(R, T)\frac{b'r - b}{2r^2\left(1 - \frac{b}{r}\right) + \frac{2f_R'(R, T)}{r}} + f_R''(R, T)\right]. \tag{15}$$

The above mentioned system of equations is not easy to solve for ρ, p_r and p_t as it has higher order derivatives with a number of unknowns. To make these calculations easy, we choose the split-up scenario which is $f(R, T) = f_2(T) + f_1(R)$. By considering $f_2(T) = \lambda T$ with coupling constant λ. Then, by incorporating $f(R, T)$ with split form in equations (10)–(12), we have the following final version of the field equations

$$\rho = \frac{b'f_R}{r^2(8\pi + \lambda)}, \tag{16}$$

$$p_r = -\frac{bf_R}{r^3(8\pi + \lambda)} + \frac{f_R'}{2r^2(8\pi + \lambda)}(-b + b'r) - \left(1 - \frac{b}{r}\right)\frac{f_R''}{8\pi + \lambda}, \tag{17}$$

$$p_t = -\frac{f_R'}{r(8\pi + \lambda)}\left(1 - \frac{b}{r}\right) + \frac{f_R}{2r^3(8\pi + \lambda)}(-b + b'r). \tag{18}$$

Now, we are going to consider a nonlinear function for $f_1(R)$, which is defined as:

$$f_1(R) = R + \gamma R^2, \tag{19}$$

where γ is the model parameter. By taking $\gamma = \lambda = 0$, we get the GR case. In the current study, we try to check the difference in the behavior of ECs between $f(R, T)$ and GR cases. The adopted model like $f(R, T) = f_2(T) + f_1(R) = R + \gamma R^2 + \lambda T$ involves a particular case of well-known Starobinsky model [58] with matter coupling. It is an interesting to mention that, in the Starobinsky model $R + \gamma R^2$, a maximum value of configuration mass or beyond is reached when the value of the parameter γ is chosen to be negative. But, this leads to an issue; specifically, the Ricci scalar performs a damped oscillation. On the other hand, the Ricci scalar smoothly decreases to zero as we approach towards infinity for positive values of parameter γ. The other involve matter coupling parameter like λ can be chosen freely. In the current study, we shall fix its positive values.

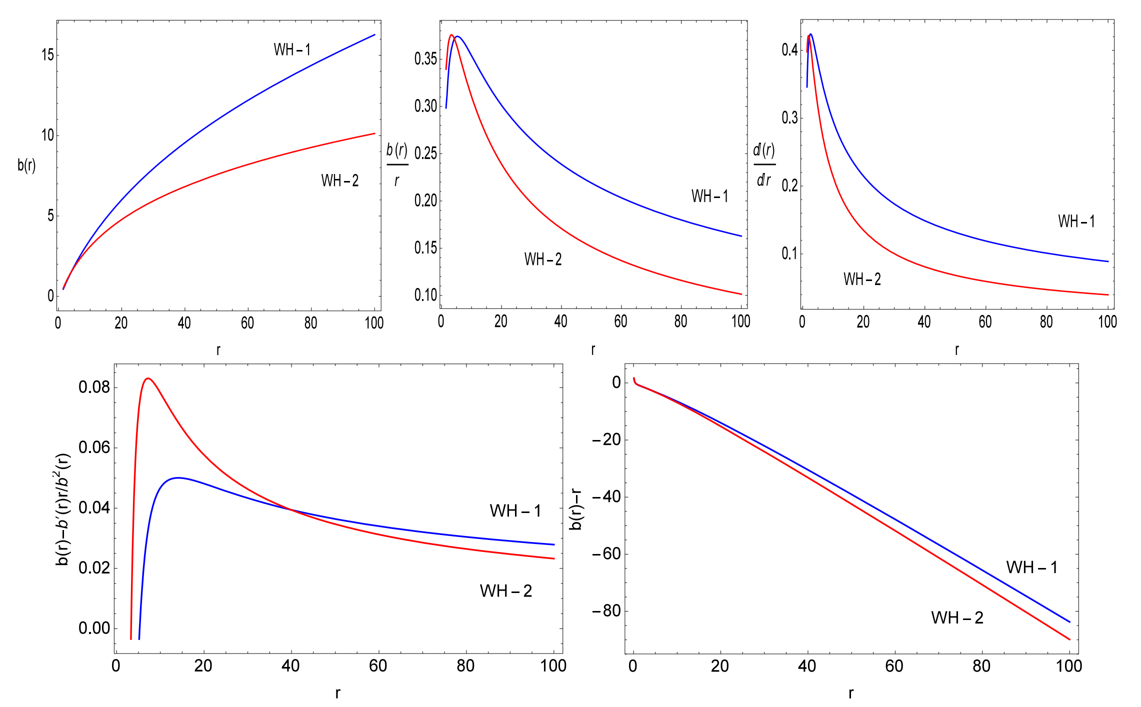

Figure 1. Shows the evolution of WH properties with $L = 0.50, a_0 = 0.20,\ a_1 = 0.30,\ a_2 = 0.40$, and $n = 0.7$.

2.1. New wormhole solutions

In this section, we shall discuss the Morris and Thorne [2] conditions for two new generic shape functions. The radial coordinate r varies between $r_0 \leqslant r < \infty$, with radius of throat r_0. In addition, the shape function $b(r)$ necessity follows traversable WH throat condition: at the throat i.e., at $r = r_0$, $b(r_0) = r_0$, and for $r > r_0$ we have $1 - \frac{b(r)}{r} > 0$. For the flaring-out condition, the following restriction must be confirmed as $b'(r_0) < 1$. To acquire the asymptotically flat regions, the following expression: $b(r)/r \to 0$ as $r \to \infty$ should be satisfied. Now, we consider two most generic shape functions, which are expressed as

$$\begin{aligned} b(r) = \frac{1}{2n^2}(2\ln(r_0)(n(a_0 + a_1) - a_0\ln(r)) - 2n\ln(r)(a_0 + a_1) + 2n^2(a_0 + a_1 + a_2) \\ + a_0\ln(r^2) + a_0\ln(r_0^2)), \end{aligned} \tag{20}$$

$$\begin{aligned} b(r) = \frac{2}{2L^2}((a_0(2n^2(r^L - r_0^L)^2 - 2Ln(r^L - r_0^L) + L^2) + L(a_1(-2nr^L + 2nr_0^L + L) + a_2L)) \\ + L(\ln(r) - \ln(r_0))(a_0L(\ln(r) - \ln(r_0)) - 2(a_0(2n(r_0^L - r^L) + L) + a_1L))), \end{aligned} \tag{21}$$

where $0.1 < L < 1.0, 0.1 < a_0 < a_1 < a_2 < 0.5$, and $-2 < n < 2$. According to Morris and Thorne [2], our presented shape functions meet the essential conditions for the existence of a wormhole. Both the chosen shape functions are observed as positive with increasing behavior, which can be confirmed from the figure 1. The derivative of both the WHs models with respect to the radial coordinate, i.e., $\frac{db}{dr}$ is noticed as less than one, which affirmed the flaring out condition. Figure 1 presents all the required conditions graphically under the particular values of the involved physical parameters.

3. Energy conditions

The ECs are the most suitable approach to validate the physically acceptable model. These violations of such ECs show the occurrence of exotic matter (matter with exotic nature). There are four well-known ECs named weak (WEC), null (NEC), dominant (DEC) and strong (SEC). For physically acceptable WH mode, the null and weak ECs must be violated. Due to the presence of normal matter distributions, such as are verified for the positive behavior of energy density as well as pressure in general relativity and $f(R, T)$ gravity. For WH configuration, we will check the null and weak ECs which are necessary for the physical acceptability of the WH structure. Mathematically, these conditions can be defined as

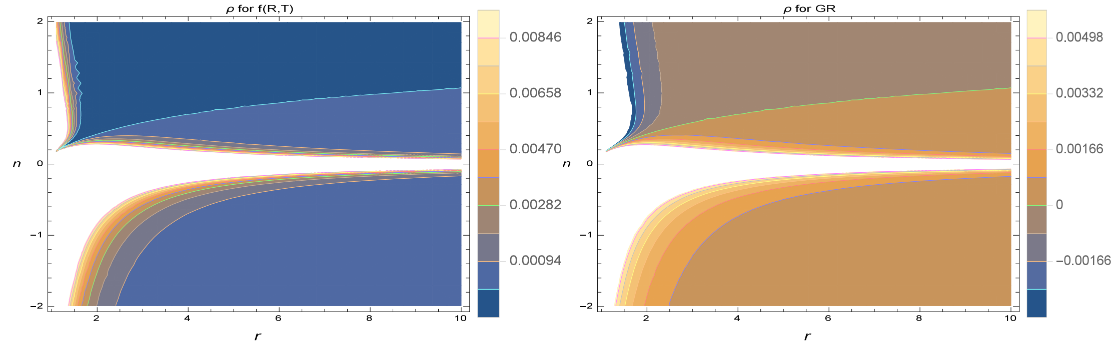

Figure 2. Plots of ρ for $f(R, T)$ gravity (Left) and GR (right) for first specific shape function by equation (19) with $L = 0.50$, $a_0 = 0.20$, $a_1 = 0.30$, $a_2 = 0.40$, $\gamma = 0.75$ and $\lambda = 0.5$.

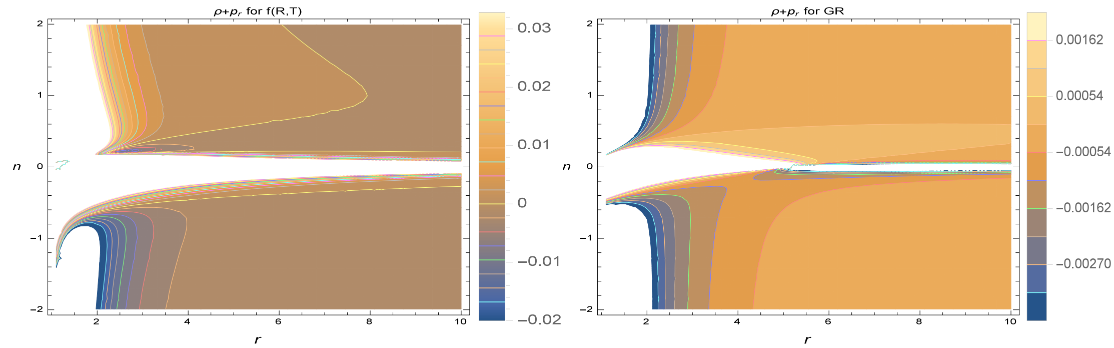

Figure 3. Plots of $\rho + p_r$ for $f(R, T)$ gravity (Left) and GR (right) for first specific shape function by equation (19) with $a_0 = 0.20$, $a_1 = 0.30$, $a_2 = 0.40$, $\gamma = 0.75$ and $\lambda = 0.5$.

$$NEC \Leftrightarrow T_{\gamma\xi}k^{\gamma}k^{\xi} \geqslant 0, \qquad WEC \Leftrightarrow T_{\gamma\xi}V^{\gamma}V^{\xi} \geqslant 0,$$
$$SEC \Leftrightarrow \left(T_{\gamma\xi} - \frac{T}{2}g_{\gamma\xi}\right)V^{\gamma}V^{\xi} \geqslant 0, \; DEC \Leftrightarrow T_{\gamma\xi}V^{\gamma}V^{\xi} \geqslant 0,$$

where V^{γ} and k^{γ} are represent timelike and null vectors, respectively. In terms of energy density and pressure, we can write

$$\begin{aligned} NEC &: \rho + p_r \geqslant 0, \quad p_t + \rho \geqslant 0,\\ WEC &: p_r + \rho \geqslant 0, \quad \rho \geqslant 0, \quad p_t + \rho \geqslant 0,\\ SEC &: p_r + \rho \geqslant 0, \quad 2p_t + \rho + p_r \geqslant 0, \quad p_t + \rho \geqslant 0,\\ DEC &: -|p_r| + \rho \geqslant 0, \quad \rho \geqslant 0, \quad -|p_t| + \rho \geqslant 0. \end{aligned}$$

Now, we consider two new generic shape functions to investigate the existence of the WH. For the first specific shape function by equation (19) ECs are presented in figures 2–7. For the second specific shape function by equation (21) ECs are graphically plotted in figures 8–13. The energy density is observed positive in all cases under both specific shape functions. The NEC and SEC are also violated in both $f(R, T)$ gravity and GR case. The violating behavior of NEC is necessary to check the presence of exotic matter. It is found that NEC and WEC are violated which represents the existence of exotic matter.

4. Thin-shell around wormholes structure

Here, we consider the exterior manifold $(+)$ as Schwarzschild BH and inner manifold $(-)$ as a traversable WH with two different choices of shape functions. Then, we explore the effects of shape function as well as physical parameters on the stable configuration of thin-shell through linearized radial perturbation. We want to build a thin shell around WH solutions using two types of shape functions in the context of $f(R, T)$ gravity. Mathematically, we can write

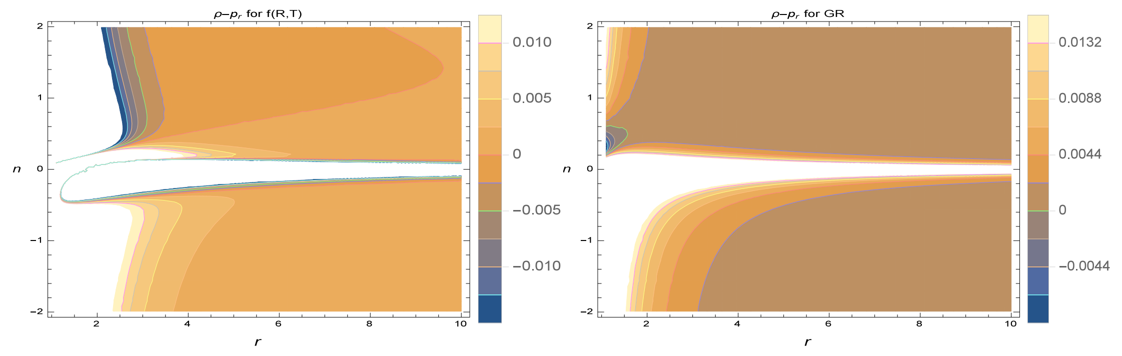

Figure 4. Plots of $\rho - p_r$ for $f(R, T)$ gravity (Left) and GR (right) for first specific shape function by equation (19) with $a_0 = 0.20$, $a_1 = 0.30$, $a_2 = 0.40$, $\gamma = 0.75$ and $\lambda = 0.5$.

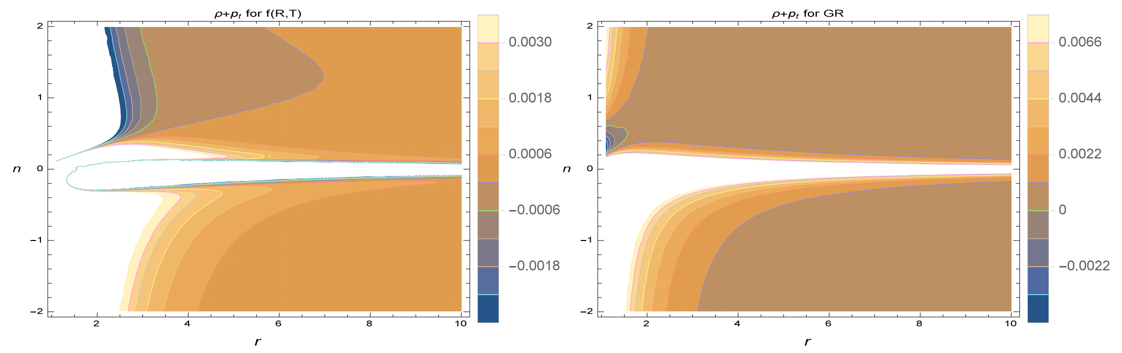

Figure 5. Plots of $\rho + p_t$ for $f(R, T)$ gravity (Left) and GR (right) for first specific shape function by equation (19) with $a_0 = 0.20$, $a_1 = 0.30$, $a_2 = 0.40$, $\gamma = 0.75$ and $\lambda = 0.5$.

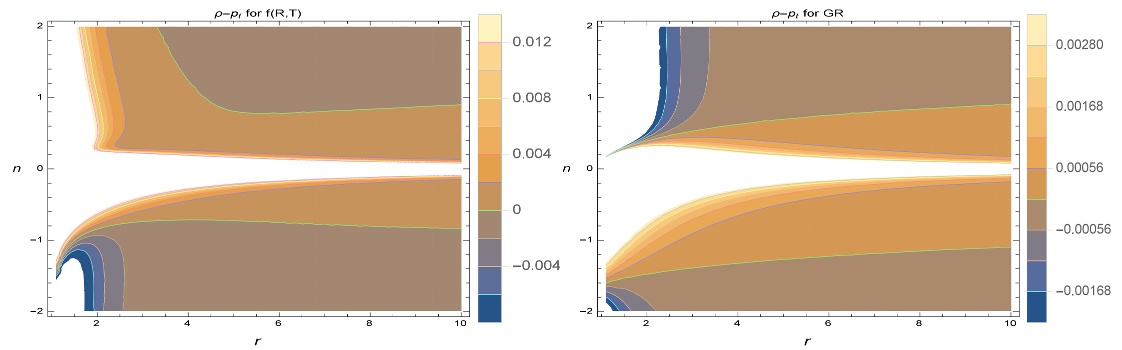

Figure 6. Plots of $\rho - p_t$ for $f(R, T)$ gravity (Left) and GR (right) for first specific shape function by equation (19) with $a_0 = 0.20$, $a_1 = 0.30$, $a_2 = 0.40$, $\gamma = 0.75$ and $\lambda = 0.5$.

$$ds_+^2 = -\Pi_+(r_+)^{-1}dr_+^2 - r_+^2 d\theta_+^2 - r_+^2 \sin^2\theta_+ d\phi_+^2 + \Pi_+(r_+)dt_+^2, \tag{22}$$

the metric function of outer (+) manifold is given as

$$\Pi_+(r_+) = -\frac{2m}{r_+} + 1, \tag{23}$$

In the Schwarzschild solution, the mass m only appears as an integration constant. By considering WH as a interior manifold (-), we can write

$$ds_-^2 = -e^{2\phi(r_-)}dt_-^2 + r_-^2 d\theta_-^2 + \frac{dr_-^2}{\Pi_-(r_-)} + r_-^2 sin^2\theta_- d\phi_-^2, \tag{24}$$

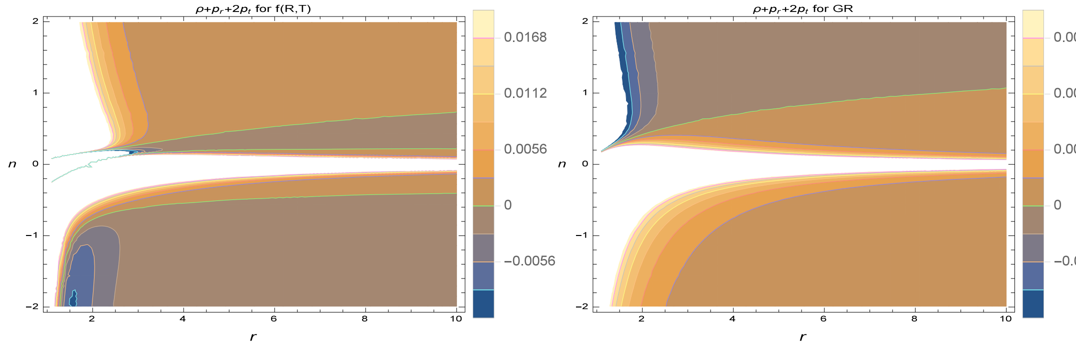

Figure 7. Plots of $\rho + p_r + 2p_t$ for $f(R, T)$ gravity (Left) and GR (right) for first specific shape function by equation (19) with $a_0 = 0.20,\ a_1 = 0.30,\ a_2 = 0.40, \gamma = 0.75$ and $\lambda = 0.5$.

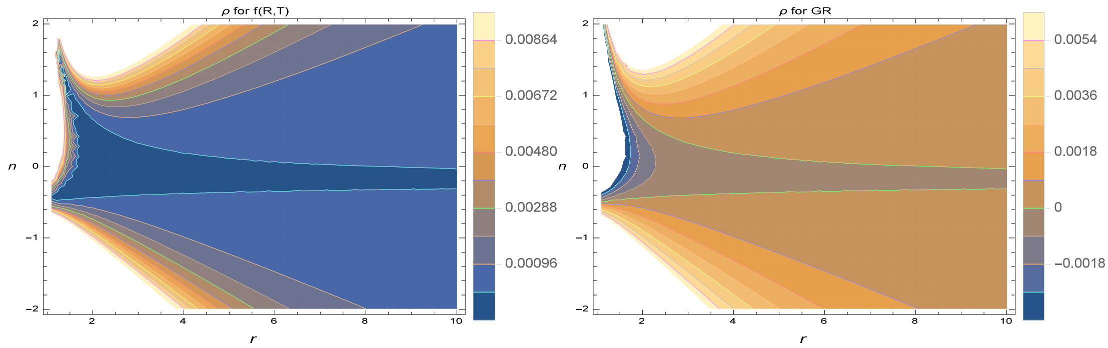

Figure 8. Plots of ρ for $f(R, T)$ gravity (Left) and GR (right) for second specific shape function by equation (21) with $L = 0.50$, $a_0 = 0.20,\ a_1 = 0.30,\ a_2 = 0.40, \gamma = 0.75$ and $\lambda = 0.5$.

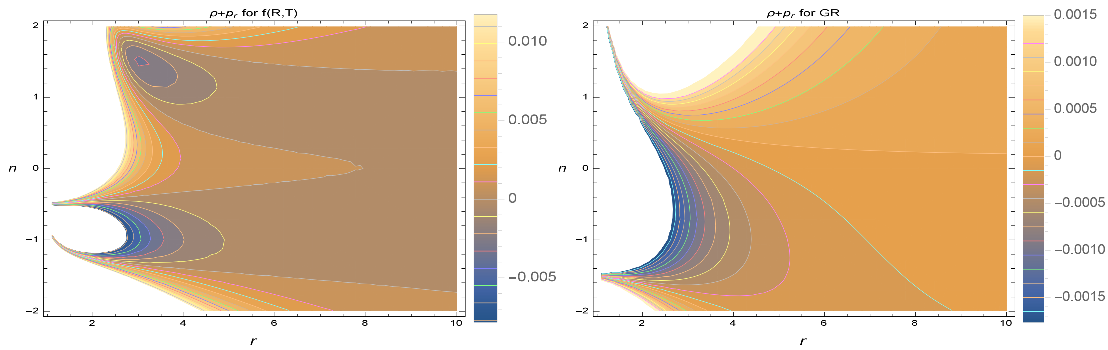

Figure 9. Plots of $\rho + p_r$ for $f(R, T)$ gravity (Left) and GR (right) for second specific shape function by equation (21) with $L = 0.50$, $a_0 = 0.20,\ a_1 = 0.30,\ a_2 = 0.40, \gamma = 0.75$ and $\lambda = 0.5$.

where

$$\Pi_{-}(r_{-}) = -\frac{b(r_{-})}{r_{-}} + 1. \tag{25}$$

Visser developed the use of a cut-and-paste approach to creating a thin-shell by combining two identical copies of BH spacetimes at a hypersurface. This technique is used in the current paper to create the geometry of the thin-shell surrounding WH spacetime. For this purpose, we cut this spacetime into the following regions as

$$\mathcal{M}^{\pm} = \{r^{\pm} \leqslant x,\ x > r_h\}, \tag{26}$$

where x is known as the radius of the thin-shell and r_h represents the position of the event horizon of Schwarzschild BH. The interior WH geometry and exterior BH spacetime are connected at (2+1)-dimensional manifold referred to as hypersurface given as

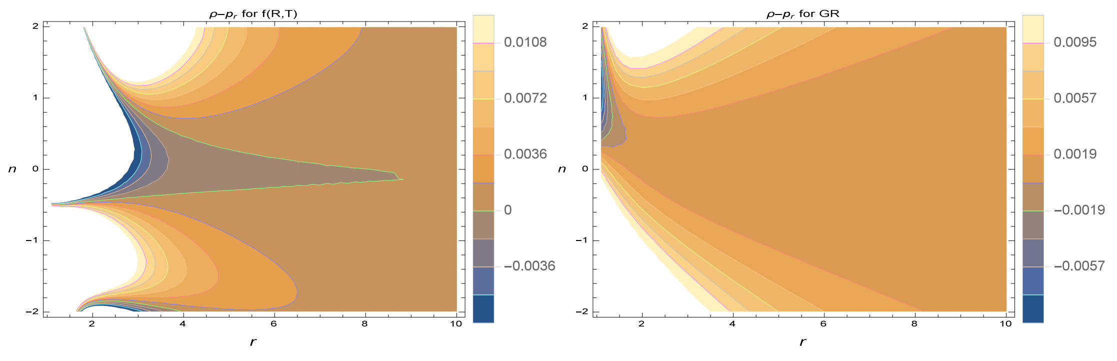

Figure 10. Plots of $\rho - p_r$ for $f(R, T)$ gravity (Left) and GR (right) for second specific shape function by equation (21) with $L = 0.50$, $a_0 = 0.20,\ a_1 = 0.30,\ a_2 = 0.40, \gamma = 0.75$ and $\lambda = 0.5$.

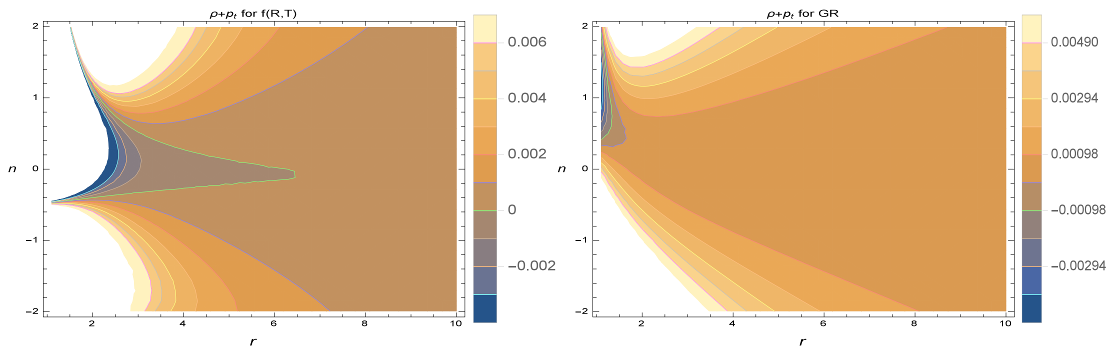

Figure 11. Plots of $\rho + p_t$ for $f(R, T)$ gravity (Left) and GR (right) for second specific shape function by equation (21) with $L = 0.50$, $a_0 = 0.20,\ a_1 = 0.30,\ a_2 = 0.40, \gamma = 0.75$ and $\lambda = 0.5$.

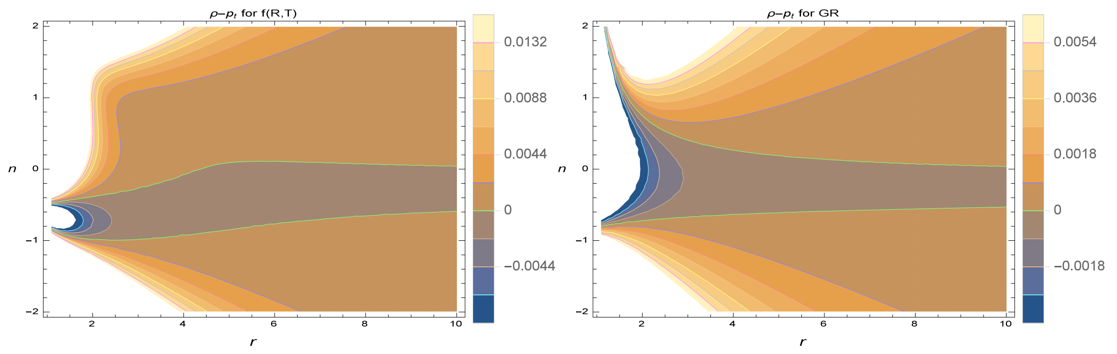

Figure 12. Plots of $\rho - p_t$ for $f(R, T)$ gravity (Left) and GR (right) for second specific shape function by equation (21) with $L = 0.50$, $a_0 = 0.20,\ a_1 = 0.30,\ a_2 = 0.40, \gamma = 0.75$ and $\lambda = 0.5$.

$$\Sigma = \{r^{\pm} = x,\ x > r_h\}. \tag{27}$$

This procedure gives a unique regular manifold and mathematically it can be expressed as $\mathcal{M} = \mathcal{M}^{-} \cup \mathcal{M}^{+}$. It's worth noting that the developed structure's event horizon and singularity can be avoided by choosing a shell radius bigger than the Schwarzschild BH's event horizon radius. According to the Darmois-Israel formalism, the coordinates of considered manifolds and hypersurface are in the following form $y_{\pm}^{\gamma} = (t_{\pm},\ r_{\pm},\ \theta_{\pm},\ \phi_{\pm})$ and $\eta^{i} = (\tau, \theta, \phi)$, respectively. Here τ represents the proper time over the hypersurface. These coordinate systems are related to one another by using the following coordinate transformation

$$g_{ij} = \frac{\partial y^{\gamma}}{\partial \eta^{i}} \frac{\partial y^{\beta}}{\partial \eta^{j}} g_{\gamma\beta}. \tag{28}$$

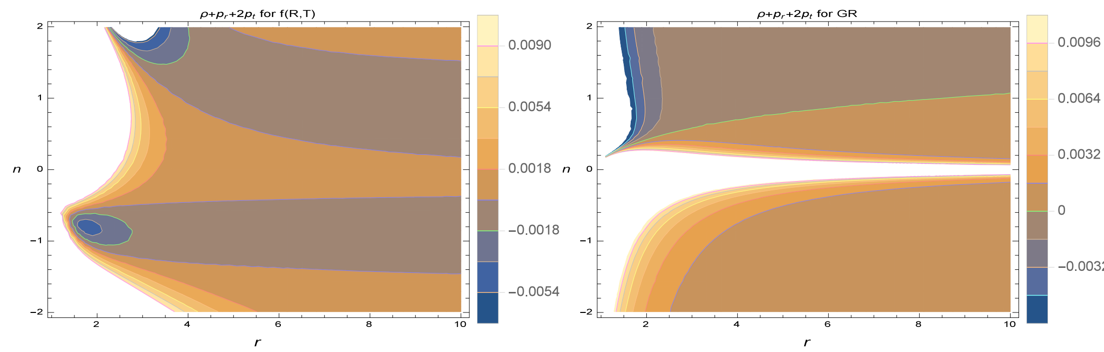

Figure 13. Plots of $\rho + p_r + 2p_t$ for $f(R, T)$ gravity (Left) and GR (right) for second specific shape function by equation (21) with $L = 0.50, a_0 = 0.20,\ a_1 = 0.30,\ a_2 = 0.40, \gamma = 0.75$ and $\lambda = 0.5$.

The respective parametric equation for the hypersurface is defined as

$$\Sigma\colon R(r,\,\tau) = r - x(\tau) = 0.$$

At hypersurface, the reduced form of Einstein field equations (Lanczos equations) is used to analyze the physical properties of matter distributions are given as

$$S^{\alpha}_{\beta} = \frac{1}{8\pi}(\delta^{\alpha}_{\beta}\zeta^{\gamma}_{\gamma} - \zeta^{\alpha}_{\beta}), \tag{29}$$

where $\zeta_{\alpha\beta} = K^{+}_{\alpha\beta} - K^{-}_{\alpha\beta}$ and $K^{-}_{\alpha\beta}$ represents the components of extrinsic curvature. For perfect fluid distribution, the stress-energy tensor is expressed as $S^{\alpha}{}_{\beta} = diag\,(\rho,\ p,\ p)$. The surface density and pressure at Σ is denoted with ρ and p, respectively. The extrinsic curvature of the interior and exterior geometries are defined as

$$K^{\pm}_{\alpha\beta} = -n^{\pm}_{\mu}\left[\frac{\partial^2 y^{\mu}_{\pm}}{\partial\eta^{\alpha}\eta^{\beta}} + \Gamma^{\mu}_{\lambda\nu}\left(\frac{\partial y^{\lambda}_{\pm}}{\partial\eta^{\alpha}}\right)\left(\frac{\partial y^{\nu}_{\pm}}{\partial\eta^{\beta}}\right)\right], \tag{30}$$

where $n^{\mu}_{\pm}$ is denoted as unit normals. By using Lanczos equations, we get

$$\sigma = -\frac{[K^{\theta}_{\theta}]}{4\pi} = -\frac{\sqrt{\dot{x}^2 - \frac{2m}{x} + 1} - \sqrt{-\frac{b(x)}{x} + \dot{x}^2 + 1}}{4\pi x}, \tag{31}$$

$$p = \frac{[K^{\theta}_{\theta}] + [K^{\tau}_{\tau}]}{8\pi} = \frac{1}{8\pi x}\left\{\frac{x(b'(x) - 2(\dot{x}^2 + \ddot{x}x + 1)) + b(x)}{x\sqrt{-\frac{b(x)}{x} + \dot{x}^2 + 1}} + \frac{2(\dot{x}^2x + \ddot{x}x^2 + x - m)}{x\sqrt{\dot{x}^2 - \frac{2m}{x} + 1}}\right\}, \tag{32}$$

while

$$\sigma + 2p = \frac{b'(x)\sqrt{\dot{x}^2 - \frac{2m}{x} + 1} - (\dot{x}^2 + 2\ddot{x}x + 1)\left(\sqrt{\dot{x}^2 - \frac{2m}{x} + 1} - \sqrt{-\frac{b(x)}{x} + \dot{x}^2 + 1}\right)}{4\pi x\sqrt{-\frac{b(x)}{x} + \dot{x}^2 + 1}\sqrt{\dot{x}^2 - \frac{2m}{x} + 1}}, \tag{33}$$

where the proper time derivative is represented with overdot. Now, it is assumed that the thin-shell of the developed geometry does not move along its radial direction at equilibrium shell radius x_0. Therefore, it is interesting to mention that the proper time derivative of shell radius vanish, i.e., $\dot{x_0} = 0 = \ddot{x_0}$. Hence, we have

$$\sigma_0 = -\frac{1}{4\pi x_0}\left\{\sqrt{-\frac{2m}{x_0} + 1} - \sqrt{-\frac{b(x_0)}{x_0} + 1}\right\},$$

$$p_0 = \frac{1}{8\pi x_0^2}\left\{\frac{x_0(b'(x_0) - 2) + b(x_0)}{\sqrt{1 - \frac{b(x_0)}{x_0}}} + \frac{2(x_0 - m)}{\sqrt{1 - \frac{2m}{x_0}}}\right\}, \tag{34}$$

and

$$\sigma_0 + 2p_0 = \frac{b'(x_0)\sqrt{1 - \frac{2m}{x_0}} + \sqrt{1 - \frac{b(x_0)}{x_0}} - \sqrt{1 - \frac{2m}{x_0}}}{4\pi x_0\sqrt{1 - \frac{b(x_0)}{x_0}}\sqrt{1 - \frac{2m}{x_0}}}, \tag{35}$$

where density and pressure at equilibrium position are denoted with σ_0 and p_0, respectively.

It is noted that $\sigma_0 < 0$ leads to the violation of weak as well as dominant energy constraints. Such violations indicate that the thin shell around WH is filled with exotic matter. Such type of distributions at thin-shell produce repulsion against collapse and also help to keep it open. As a result, the created structure is physically suitable for observer mobility inside this configuration.

5. Stability analysis through radial linear perturbation

Now, we want to use linearized radial perturbation at $x = x_0$ to investigate the stable configuration of a developed thin-shell around WH geometry. We get the equation of motion of the shell from equation (31) as follows:

$$\dot{x}^2 + V(x) = 0, \tag{36}$$

the thin-shell effective potential function is denoted with $V(x)$. It is defined as

$$V(x) = \frac{mb(x)}{16\pi^2x^4\sigma^2} - \frac{b(x)^2}{64\pi^2x^4\sigma^2} - \frac{b(x)}{2x} - \frac{m^2}{16\pi^2x^4\sigma^2} - 4\pi^2x^2\sigma^2 - \frac{m}{x} + 1. \tag{37}$$

It is worthwhile that the components of stress energy tensor follows the energy conservation constraints as

$$p\frac{d}{d\tau}(4\pi x^2) + \frac{d}{d\tau}(4\pi x^2\sigma) = 0, \tag{38}$$

which turns out to be

$$\sigma' = -\frac{2(\sigma + p(\sigma))}{x}. \tag{39}$$

We employ Taylor series to expand the effective potential up to second order terms around the equilibrium shell radius for stability analysis.

$$V(x) = V(x_0) + (x - x_0)V'(x_0) + \frac{1}{2}(x - x_0)^2V''(x_0) + O[(x - x_0)^3]. \tag{40}$$

It is noted that $V(x_0) = 0 = V'(x_0)$. Hence, we get

$$V(x) = \frac{1}{2}(x - x_0)^2V''(x_0). \tag{41}$$

In terms of energy density and pressure, thin-shell mass and its radial derivatives are given as

$$M(x_0) = 4\pi x_0^2\sigma_0, \qquad M'(x_0) = -8\pi x_0 p_0, \qquad M''(x_0) = -8\pi p_0 + 16\pi\xi_0^2(\sigma_0 + p_0),$$

here $\xi_0^2 = dp/d\sigma|_{x=x_0}$ is a EoS parameter. So, we get

$$\begin{aligned}V''(x_0) = &-\frac{1}{2x_0^4M^4}\{-x_0^4M(2m - b(x_0))(M''(2m - b(x_0)) - 4M'b'(x_0))\\ &+ x_0^4M^2((b(x_0) - 2m)b''(x_0) + b'(x_0)^2)\\ &+ x_0M^4(x_0(x_0b''(x_0) - 2b'(x_0) + (M')^2) + 2b(x_0) + 4m) + 3x_0^4(M')^2(b(x_0) - 2m)^2\\ &+ x_0M^5(x_0M'' - 4M') + 3M^6\}.\end{aligned} \tag{42}$$

The second derivative of the potential function at $x = x_0$ may be used to illustrate thin-shell stability as follows: [15]

(i) For stable $\Rightarrow$ $V''(x_0) > 0$,

(ii) For unstable $\Rightarrow$ $V''(x_0) < 0$,

(iii) Unpredictable $\Rightarrow$ $V''(x_0) = 0$.

We'll look at the first scenario to see if the established structure is stable. Hence, equation (42) becomes

$$\begin{aligned}&-(-\sigma_0(2m - b(x_0))(32\pi x_0p_0b'(x_0) + (2m - b(x_0))(16\pi\xi_0^2(p_0 + \sigma_0) - 8\pi p_0)) + 48\pi p_0^2(b(x_0) - 2m)^2\\ &+4\pi x_0^2\sigma_0^2((b(x_0) - 2m)b''(x_0) + b'(x_0)^2) + 64\pi^3x_0^3\sigma_0^4(x_0^2b''(x_0) - 2x_0b'(x_0) + 2b(x_0) + 64\pi^2x_0^3p_0^2 + 4m)\\ &+2048\pi^5x_0^6\sigma_0^5((2\xi_0^2 + 3)p_0 + 2\xi_0^2\sigma_0) + 3072\pi^5x_0^6\sigma_0^6)(128\pi^3x_0^6\sigma_0^4)^{-1} > 0,\end{aligned} \tag{43}$$

Stability constraints (43) can also be written in the following format:

$$V''(x_0) > 0, \quad \Rightarrow \quad \lambda(x_0)\xi_0^2 - \mathcal{E}_0 > 0. \tag{44}$$

Here, the coefficient of EoS parameter is denoted with $\lambda(x_0) = \lambda_0$ and remaining terms are named as $\mathcal{E}(x_0) = \mathcal{E}_0$.

The geometrical configuration of thin-shell is explored by using stable regions which can expressed as

(i) For $\lambda_0 < 0 \Rightarrow \ \xi_0^2 < \mathcal{E}_0/\lambda_0$:

(ii)For $\lambda_0 > 0 \Rightarrow \ \xi_0^2 > \mathcal{E}_0/\lambda_0$,

where

$$\begin{aligned}\mathcal{E}_0 &= b(x_0)(8(mp_0(6p_0 + \sigma_0) - 4\pi^2 x_0^3\sigma_0^4) - x_0\sigma_0(x_0\sigma_0 b''(x_0) + 8p_0 b'(x_0)))\\ &\quad + x_0\sigma_0(2x_0\sigma_0 b''(x_0)(m - 8\pi^2 x_0^3\sigma_0^2) + b'(x_0)(-x_0\sigma_0 b'(x_0) + 32\pi^2 x_0^3\sigma^3 + 16mp_0)) - 2p_0 b(x_0)^2(6p_0 + \sigma_0)\\ &\quad - 8(32\pi^4 x_0^6\sigma_0^4(4p_0^2 + 6p_0\sigma_0 + 3\sigma_0^2) + 8\pi^2 x_0^3 m\sigma_0^4 + m^2 p_0(6p_0 + \sigma_0)),\\ \lambda_0 &= 4\sigma_0(p_0 + \sigma_0)(4mb(x_0) - b(x_0)^2 + 256\pi^4 x_0^6\sigma_0^4 - 4m^2).\end{aligned}$$

Stability regions are used to investigate the properties of thin-shell surrounding WH geometry for both the shape functions given as:

$$\begin{aligned}b_1(x_0) &= \frac{1}{2n^2}(2\ln(r_0)(-a_0\ln(x_0) + n(a_0 + a_1)) - 2n\ln(x_0)(a_0 + a_1)\\ &\quad + a_0\ln(x_0^2) + a_0\ln(r_0^2) + 2n^2(a_0 + a_1 + a_2)),\\ b_2(x_0) &= \frac{2}{2L^2}((a_0(2n^2(x_0^L - r_0^L)^2 - 2Ln(x_0^L - r_0^L) + L^2)\\ &\quad + L(a_1(-2nx_0^L + 2nr_0^L + L) + a_2 L)) + L(\ln(x_0) - \ln(r_0))\\ &\quad \times (a_0 L(\ln(x_0) - \ln(r_0)) - 2(a_0(2n(r_0^L - x_0^L) + L) + a_1 L))).\end{aligned}$$

Now, we consider both shape function to discuss stability regions of developed structure. For this purpose, we use $\mathcal{E}_0/\lambda_0$ to obtain the stability regions for $a_0 = 0.2, a_1 = 0.3, a_3 = 0.4, n = 9, r_0 = 0.1, m = 0.5$.

- For the first case of shape function, figures 14 and 15 express the graphical behavior of $\mathcal{E}_0/\lambda_0$. The brown region represents the stable regions and light gray and white regions show unstable regions for suitable choices of physical parameters. Figure 14 shows the stable regions for different values of n and noted that the position of an event horizon is decreased as n increases. figure 15 shows the effects of the mass of the Schwarzschild BH on the stable regions of the shell. It is noted that stable regions are found for every suitable value of physical parameters.
- For the second case of shape function, we explore characteristics of geometrical structure for different values of m and integration constant L as shown in figures 16 and 17. It is found that the number of an expected event horizon increases for the second shape function as compared to $b_1(x_0)$. It represents the possibility of stable/unstable regions throughout the domain of shell radius for suitable values of physical parameters.

6. Concluding remarks

However, the recent observational restrictions have not recognized stable WHs with traversability conditions. The WH geometry has a critical role in numerous significant problems in the framework of gravitation. WH might define our only prospect for interstellar in the far future. Most WH solutions are considered black hole mimickers and the outstanding evolution in the past few years in our competence in revealing the strong gravity region of black holes has reinvigorated new studies to check whether astrophysical blacks are the mouths of WHs towards the regions of the Universe. Many works have been done in the framework of modified theories of gravity to check the nature of the involved matters regarding WH existence. Lobo and his coauthors [59–62] presented some most general conditions in the background of different modified gravity, in which the matter threading the wormhole throat satisfies all of the energy conditions. They also provided the reason for it that the higher order curvature terms, which may be interpreted as a gravitational fluid, support these nonstandard wormhole geometries. In the current study, we have checked the effect of two new shape functions on the energy conditions in the background of $f(R, T)$ and GR cases. In the current analysis, we have chosen two generic new shape functions for WH geometry. The energy conditions, like, NEC, WEC, DEC, and SEC have been checked by using the two new generic shape functions. The investigation regarding the behavior of energy conditions has confirmed the violation of the energy conditions in both cases, i.e., $f(R, T)$ and GR case. For the traversable WH the nature of the matter, the especially exotic matter has a special role in the current study. In both cases under

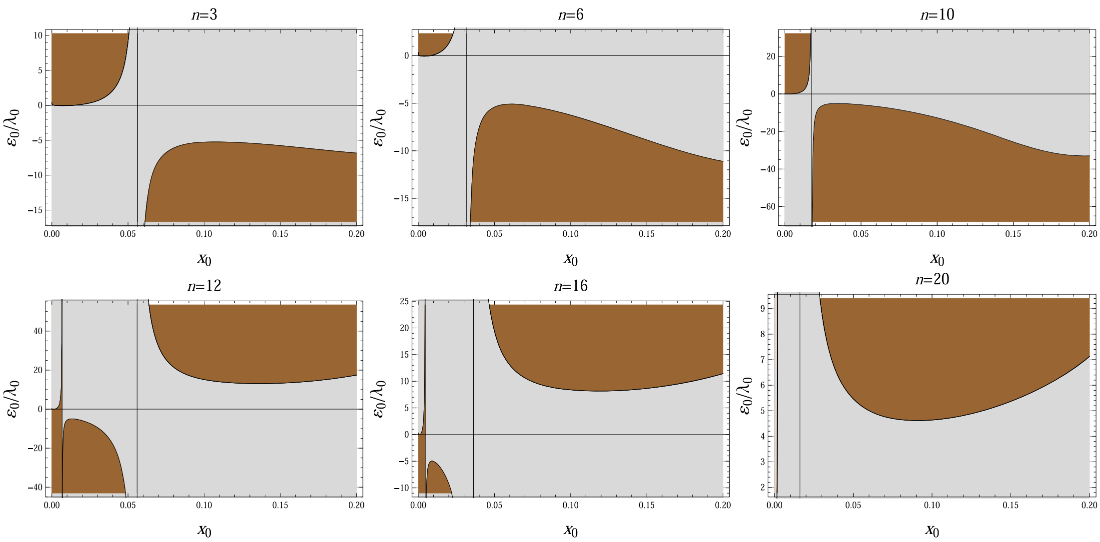

Figure 14. Stable regions for the choice of first shape function (case(i)) for different values of n. The straight line shows the position of expected event horizon of the developed structure. Stable regions are denoted with brown color while light gray and white colors show unstable regions.

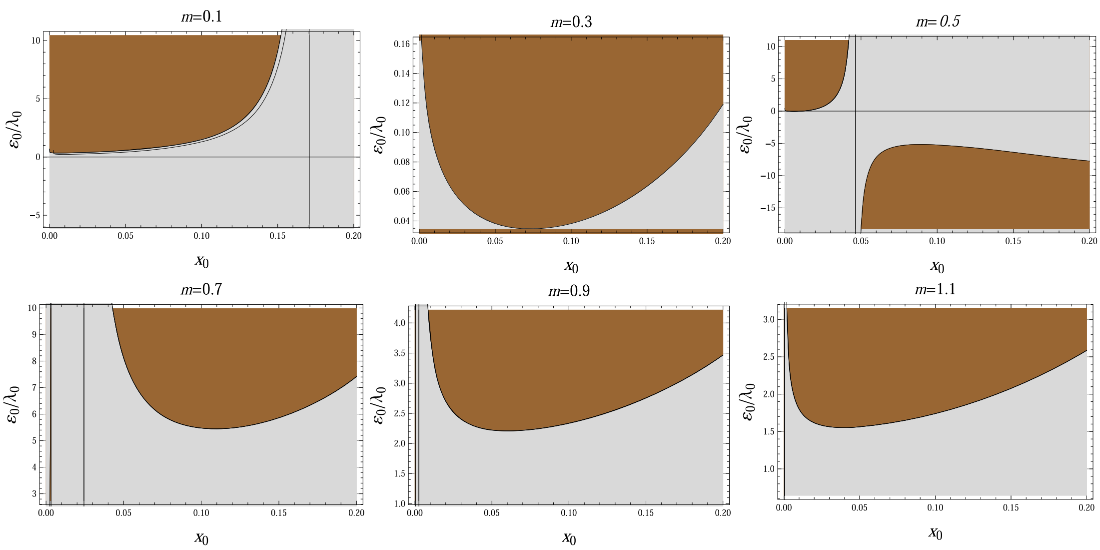

Figure 15. Stable regions for the choice of first shape function (case(i)) for different values of m.

both WH models the violating behavior of energy conditions, especially NEC has confirmed the presence of exotic matter. Some outcomes of this study are listed below:

- All the required necessary conditions for WH stable solutions are provided in figure 1, including flaring out and flatness conditions.
- The energy density, which is provided in figures 2 and 8 is observed as positive in $f(R, T)$ gravity, while it is seen as negative in the partial region for GR case.
- The NEC is also discussed with graphical regions (figures 3 and 9), which is noticed with violating behavior.
- The SEC is shown graphically in figures 2 and 8, which is seen as negative in all cases and hence supports the violation.

Further, We have also examined the stability of a thin-shell around a WH geometry in the background of $f(R, T)$ gravity. We used the Schwarzschild black hole as an outside geometry and produced WH solutions with two

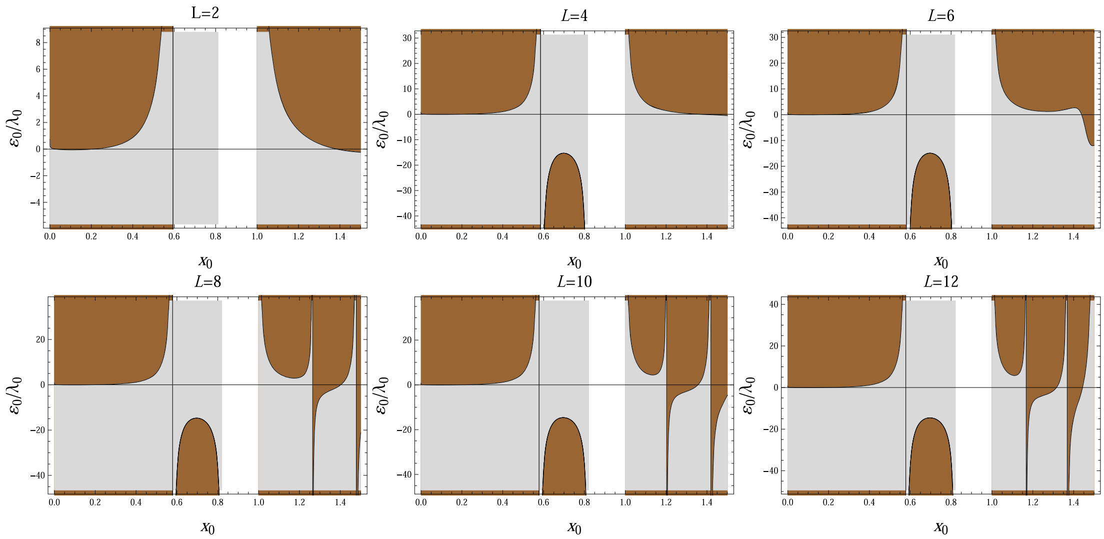

Figure 16. Stable regions for the choice of second shape function (case(ii)) for different values of L.

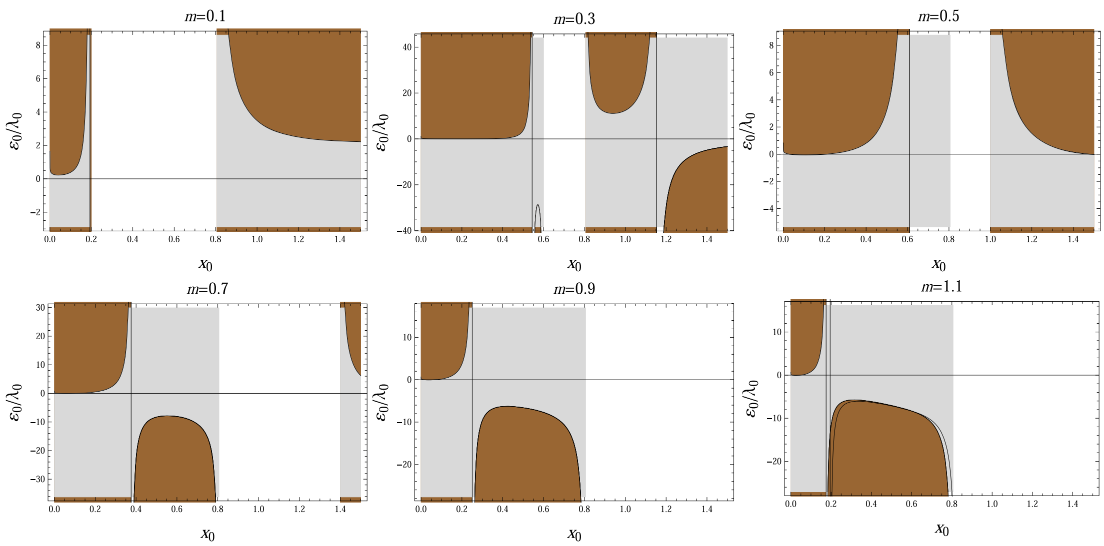

Figure 17. Stable regions for the choice of second shape function (case(ii)) for different values of m.

different shape functions as an inner manifold. The stability of thin-shell geometry surrounding WHs is explored by using linearized radial perturbation over the equilibrium position of the shell radius. It should be highlighted that stable regions are achieved for both shape functions with appropriate values of physical parameters. It is interesting to mention that the second shape function provides more possibility for stable structure comparatively $b_1(x_0)$. It is interesting to mention here that our constructed WH solutions satisfy all the required conditions that should be present for the existence of WH solutions. In $f(R, T)$ gravitational theory, we have obtained that the NEC, as well as WEC for the resulting WHs, is violated so, our results are consistent with the that discussed before [63–68].

Acknowledgments

G Mustafa is very thankful to Prof Gao Xianlong from the Department of Physics, Zhejiang Normal University, for his kind support and help during this research. Further, G Mustafa acknowledges the Grant No. ZC304022919 to support his Postdoctoral Fellowship at Zhejiang Normal University.

Data availability statement

The data generated and/or analysed during the current study are not publicly available for legal/ethical reasons but are available from the corresponding author on reasonable request.

ORCID iDs

Faisal Javed https://orcid.org/0000-0001-6970-1305
G Mustafa https://orcid.org/0000-0003-1409-2009

References

[1] Misner C W and Wheeler J A 1957 Classical physics as geometry *Ann. Phys.* **2** 525
[2] Morris M and Thorne K 1988 WHs in spacetime and their use for interstellar travel: a tool for teaching general relativity *Am. J. Phys.* **56** 395
[3] Visser M 1989 Traversable WHs: some simple examples *Phys. Rev.* D **39** 3182
Visser M 1996 *Lorentzian WHs* (AIP Press)
[4] Shinkai H and Hayward S A 2002 Fate of the first Traversible WH: black-hole collapse or inflationary expansion *Phys. Rev.* D **66** 044005
[5] Visser M, Kar S and Dadhich N 2003 Traversable wormholes with arbitrarily small energy condition violations *Phys. Rev. Lett.* **90** 201102
[6] Bouhmadi-López M, Lobo F S N and Martín-Moruno P 2014 Wormholes minimally violating the null energy condition *J. Cosm. Astrop. Phys.* **1411** 007
[7] Parsaei F and Rastgoo S 2020 Wormhole solutions with a polynomial equation-of-state and minimal violation of the null energy condition *Eur. Phys. J.* C **80** 366
[8] Perlmutter S *et al* 1998 Discovery of a supernova explosion at half the age of the universe *Nature* **391** 51
Perlmutter S *et al* 1999 Measurements of Ω and Λ from 42 high-redshift supernovae *Astrophys. J.* **517** 565
[9] Shushkov S 2005 Wormholes supported by a phantom energy *Phys. Rev.* D **71** 043520
[10] Lobo F S N 2005 Phantom energy traversable wormholes *Phys. Rev.* D **71** 084011
[11] Lobo F S N 2007 Van Der Waals Quintessence Stars *Phys. Rev.* D **75** 024023
[12] Nojiri S and Odintsov S D 2011 Unified cosmic history in modified gravity: from $F(R)$ theory to lorentz non-invariant models *Phys. Rep.* **505** 59
[13] Lobo F S N and Oliveira M A 2009 Wormhole geometries in $f(R)$ modified theories of gravity *Phys. Rev.* D **80** 104012
[14] Eiroa E F and Aguirre G F 2016 Thin-shell wormholes with charge in $F(R)$ gravity *Eur. Phys. J.* C **76** 132
[15] Övgün A and Jusufi K 2017 Stable dyonic thin-shell wormholes in low-energy string theory *Adv. High Energy Phys.* **2017** 1215254
[16] Mazharimousavia S H and Note A 2018 on thin-shell wormholes with charge in $F(R)$ -gravity *Eur. Phys. J.* C **78** 612
[17] Lobo F S N, Olmo G J, Rubiera-Garcia E O D and Rustam A 2020 Structure and stability of traversable thin-shell wormholes in Palatini $f(R)$ gravity *Phys. Rev.* D **102** 104012
[18] Lobo I P, Richarte M G, Graça J P M and Moradpour H 2020 Thin-shell wormholes in rastall gravity *Eur. Phys. J. Plus* **135** 550
[19] Hassan Z, Mandal S and Sahoo P K 2021 Traversable wormhole geometries in gravity *Forts. de Phys.* **69** 2100023
[20] Capozziello S, Luongo O and Mauro L 2021 Traversable wormholes with vanishing sound speed in $f(R)$ gravity *Eur. Phys. J. Plus* **136** 1
[21] Javed F, Mustafa G, Övgün A and Shamir M F 2021 Epicyclic frequencies and stability of thin shell around the traversable wormholes in rastall gravity *Eur. Phys. J. Plus* **61** 137
[22] Harko T, Lobo F S N, Nojiri S and Odintsov S D 2011 $f(R, T)$ gravity *Phys. Rev.* D **84** 024020
[23] Houndjo M J S 2012 Reconstruction of $f(R, T)$ gravity describing matter dominated and accelerated phases *Int. J. Mod. Phys.* D **21** 1250003
[24] Yousaf Z, Bamba K and Bhatti M Z 2016 The influence of modification of gravity on the dynamics of radiating spherical fluids *Phys. Rev.* D **93** 064059
[25] Yousaf Z, Ilyas M and Bhatti M Z 2017 Influence of modification of gravity on spherical wormhole models *Mod. Phys. Lett.* A **32** 1750163
[26] Yousaf Z, Bhatti M Z and Asad H 2022 Hyperbolically symmetric sources in $f(R, T)$ gravity *Ann. Phys.* **437** 168753
[27] Elizalde E and Khurshudyan M 2019 Wormhole models in $f(R, T)$ gravity *Int. J. Mod. Phys.* D **28** 1950172
[28] Moraes P H R S and Sahoo P K 2019 Wormholes in exponential $f(R, T)$ gravity *Eur. Phys. J.* C **79** 677
[29] Moraes P H R S, de Paula W and Correa R A C 2019 Charged wormholes in $f(R, T)$ -extended theory of gravity *Int. J. Mod. Phys.* D **28** 1950098
[30] Mandal S, Sahoo P and Sahoo P K 2020 Wormhole model with a hybrid shape function in $f(R, T)$ gravity *New Astron.* **80** 101421
[31] Sharif M and Zeeshan Gul M 2021 Viable wormhole solutions in energy-momentum squared gravity *Eur. Phys. J. Plus* **136** 503
[32] Sharif M and Ashraf K 2020 Impact of Kuchowicz metric function on gravastars in $f(R, T)$ theory *Eur. Phys. J. Plus* **135** 930
[33] Sharif M, Nawazish I and Hussain S 2020 Static wormhole solutions and Noether symmetry in modified Gauss-Bonnet gravity *Eur. Phys. J.* C **80** 783
[34] Sharif M and Ashraf K 2021 Stability of ABG thin-shell around a traversable wormhole *Int. J. Geom. Meth. Mod. Phys.* **18** 2150044
[35] Sharif M and Ashraf K 2020 Study of thin-shell around wormhole *Chin. J. Phys.* **65** 242–53
[36] Sahoo P, Moraes P H R S, Lapola M M and Sahoo P K 2021 Traversable wormholes in the traceless f(R,T) gravity *Int. J. Mod. Phys.* D **30** 2150100
[37] Mishra A K and Sharma U K 2021 Wormhole models in R^2-gravity for $f(R, T)$ theory with a hybrid shape function *Can. J. Phys.* **99** 481
[38] Shamir M F 2015 Exact solutions of Bianchi type V spacetime in $f(R, T)$ gravity *Int. J. Theor. Phys.* **54** 1304
[39] Israel W 1966 *Nuovo Cim. B Ser.* **44** 1
Israel W 1967 *ibid* **48** 463
[40] Randall L and Sundrum R 1999 *Phys. Rev. Lett.* **83** 3370
Randall L and Sundrum R 1999 *ibid.* **83** 4690
[41] Fraundiener J, Hoenselaers C and Konrad W 1990 *Class. Quant. Grav.* **7** 585

[42] Sakai N and Maeda K 1994 *Phys. Rev.* D **50** 5425
[43] Vilenkin A 1981 *Phys. Rev.* D **23** 852
Ipser J and Sikivie P 1984 *Phys. Rev.* D **30** 712
Garfinkle D and Gregory R 1990 *Phys. Rev.* D **41** 1889
[44] Brady P R, Louko J and Poisson E 1991 *Phys. Rev.* D **44** 1891
[45] Martinez E A 1996 *Phys. Rev.* D **53** 7062
[46] Mazharimousavi S H, Halilsoy M and Hamad A S N 2017 *Int. J. Mod. Phys.* D **26** 1750158
[47] LeMaitre P and Poisson E 2019 *Amer. J. Phys.* **87** 961
[48] Mazur P and Mottola E 2004 *Proc. Nat. Acad. Sci* **101** 9545
[49] Visser M and Wiltshire D L 2004 *Class. Quantum Grav.* **21** 1135
[50] Frolov V P and Novikov I D 1990 *Phys. Rev.* D **42** 1057
[51] Lobo F S N 2004 *Class. Quantum Grav.* **21** 4811
[52] Garcia N M *et al* 2012 *Phys. Rev.* D **86** 044026
[53] Forghani S D *et al* 2018 *Eur. Phys. J. Plus* **133** 497
[54] Sharif M and Ashraf K 2020 *Chin. J. Phys.* **65** 242
[55] Harko T and Lobo F S N 2010 *Eur. Phys. J.* C **70** 373
[56] Harko T and Lobo F S N 2014 *Galaxies* **2** 410
[57] Bertolami O *et al* 2008 *Phys. Rev.* D **78** 064036
[58] Starobinsky A A 1980 *Phys. Lett.* B **91** 99
[59] Lobo F S N 2012 *AIP Conference Proceedings* 1458 447
[60] Harko T, Lobo F S N, Mak M K and Sushkov S V *Phys. Rev.* D **87** 067504
[61] Böhmer C G, Harko T and Lobo F S N *Phys. Rev.* D **85** 044033
[62] Lobo F S N and Oliveira M A 2009 *Phys. Rev.* D **80** 104012
[63] Sharif M and Yousaf Z 2014 Cylindrical thin-shell wormholes in $f(R)$ gravity *Astrophys. Space Sci.* **351** 351
[64] Bhatti M Z, Yousaf Z and Ashraf S 2017 Charged black string thin-shell wormholes in modified gravity, Ann *Phys.* **383** 439
[65] Bhatti M Z, Yousaf Z and Ilyas M 2018 Existence of wormhole solutions and energy conditions in $f(R, T)$ gravity *J. Astrophys. Astron.* **39** 69
[66] Eiroa E F and Romero G E 2004 Linearized stability of charged thin-shell wormholes *Gen. Relativ. Gravit.* **36** 651
[67] Mustafa G *et al* 2022 *Fortschr. Phys.* 2200053
[68] Mustafa G *et al* 2021 *Phys. Lett.* B **821** 136612